A Novel Hybrid-Fed Patch Antenna With Pattern Diversity

Kunpeng Wei, Zhijun Zhang, *Senior Member, IEEE*, Wenhua Chen, *Member, IEEE*, and Zhenghe Feng, *Senior Member, IEEE*

***Abstract*—In this letter, a novel hybrid-fed circular patch antenna operating with TM_{11} and TM_{01} modes is presented. By making use of a hybrid feed network, the two modes can be operated at an overlapped frequency range for 2.4-GHz WLAN applications, while TM_{11} mode reveals good broadside radiation patterns and TM_{01} mode shows monopole-like radiation patterns. The proposed antenna is fabricated and tested. The measured gain for the broadside mode is 7.1–9.1 dBi from 2.16 to 2.72 GHz (23.0%), and for the conical mode 3.4–4.3 dBi from 2.14 to 2.64 GHz (20.5%). High isolation $(< -40\ \mathrm{dB})$ between the two feeding ports for the entire impedance bandwidth of the proposed antenna is achieved. The planar dual-port antenna provides different patterns and polarizations to take advantage of the pattern and polarization diversity for modern mobile communications.**

***Index Terms*—Antenna radiation patterns, microstrip antenna, pattern and polarization diversity.**

I. Introduction

DUE to the rapid development of modern wireless communication systems, multifunctional antennas with different radiation characteristics have become more and more important [1]. Moreover, multiantenna systems with diversity schemes are a promising solution, which can enhance system performance by mitigating multipath fading and increasing channel capacity. Multiantenna systems with diversity schemes also improve the utility efficiency of the limited spectra and spatial resources [2]. With low-cost fabrication, compact size, and flexible structure, microstrip patch antennas are widely used in mobile communication systems [3]. However, suffering from the disadvantages of narrow bandwidth or limited types of polarization and pattern, patch antennas are not easily applied to diversity systems. To resolve the limitations of patch antennas, various techniques for designing patch antennas with wide bandwidth or with multiple radiation patterns have been proposed [4]–[9]. For bandwidth enhancement, several broadband feeding structures have been presented, such as the L-shaped probe feeding technique [4], proximity coupling by etching an H-shaped slot [5], and the capacitive feed technique [6].

The capability of supporting multiple independent far-field radiation patterns is attractive for enhancing mobile system performance. The short-circuited ring patch (SCRP) antenna made by incorporating a shorting rod at the center of a circular patch has been thoroughly studied [7]–[9]. This geometry can be easily constructed to have the capability of supporting two independent radiation patterns: a broadside TM_{11} mode and a conical TM_{01} mode with a "monopolar" radiation pattern. Since the conical TM_{01} mode with vertical polarization can ensure adequate coverage along low elevation planes, it is very attractive for low-profile antennas. However, in conventional circular or ring patches, TM_{01} mode is a higher order mode. In order to design the antenna with the two resonant modes in the same frequency, shorting posts [10] have been added to reduce the resonant frequency of TM_{01} mode. Nevertheless, due to the large size or complex feed and matching network design, this configuration is difficult to achieve easy fabrication and mass production.

In this letter, a conformal dual-port diversity patch antenna, operating with a broadside and/or conical radiation pattern, is demonstrated for WLAN applications. The conical and broadside modes are excited separately by using a hybrid feed network. The antenna has a simple structure and a compact size with low-cost fabrication, but still shows good performance.

II. Antenna Design

For conventional circular patch antennas [6], the radiation pattern is usually fixed by the designated TM_{11} mode. However, the narrow bandwidth of these probe-fed patches are not suitable for broadband communications. The proximity coupling technique was found to be a good candidate for enhancing the bandwidth of patch antennas. At the same time, the conical TM_{01} mode with a monopole-like radiation pattern [11] has the advantage of a lower profile than the conventional quarter-wavelength monopole antenna. Nevertheless, in conventional circular patches, the TM_{01} mode is a higher order mode, so the two modes are operated at different frequencies in a conventional patch antenna. In order to design the antenna with the two resonant modes operating at the same frequency, a hybrid feed network has been utilized to excite the dual-port diversity patch antenna.

The geometry of the proposed antenna is shown in Fig. 1. The circular patch has an outer radius of R1, and the square ground plane has an area of $100 \times 100\ \mathrm{mm}^2$. The substrate consists of an air-gap layer having a thickness of h, and two Teflon

Manuscript received April 26, 2010; accepted May 18, 2010. Date of publication May 27, 2010; date of current version June 24, 2010. This work was supported in part by the National Basic Research Program of China under Contract 2009CB320205, the National High Technology Research and Development Program of China (863 Program) under Contract 2007AA01Z284, the National Natural Science Foundation of China under Contract 60771009, and the National Science and Technology Major Project of the Ministry of Science and Technology of China 2010ZX03007-001-01.

The authors are with the State Key Lab of Microwave and Communications, Department of Electronic Engineering, Tsinghua University, Beijing 100084, China (e-mail: wkp08@mails.tsinghua.edu.cn; zjzh@tsinghua.edu.cn; chenwh@mail.tsinghua.edu.cn; fzh-dee@mail.tsinghua.edu.cn).

Color versions of one or more of the figures in this letter are available online at http://ieeexplore.ieee.org.

Digital Object Identifier 10.1109/LAWP.2010.2051402

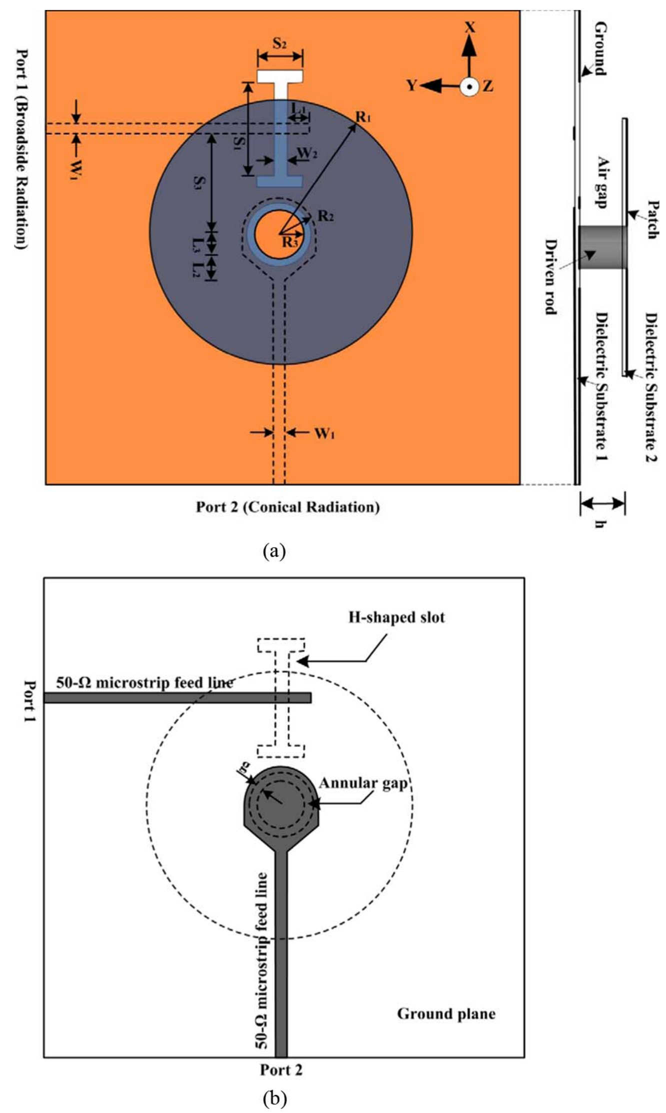

Fig. 1. Geometry of the proposed antenna. (a) Top view. (b) Hybrid feed network on the bottom layer.

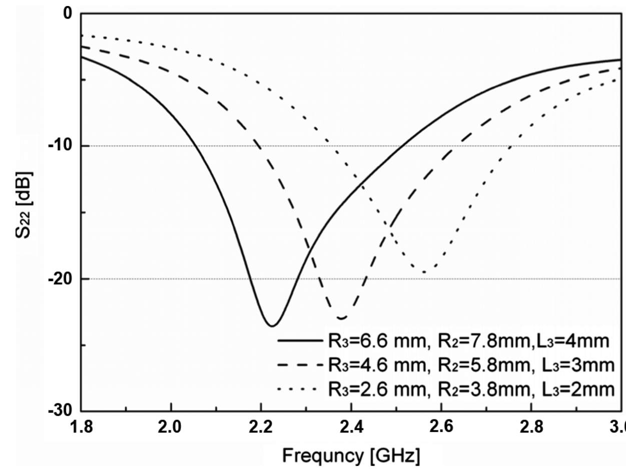

Fig. 2. S_{22} with different dimensions of the driven rod and the quasi-circular stub. Other parameters as shown in Table I.

TABLE I
DIMENSIONS OF THE PROPOSED ANTENNA (IN mm)

Parameter	R_1	W_1	W_2	L_1	L_2
Value	27	1.4	2	4	5
Parameter	S_1	S_2	S_3	h	g
Value	22	8	19.3	9.5	1

substrate layers ($\varepsilon_r = 2.65$, height $= 0.5$ mm). Port 1 for TM_{11} mode with broadside radiation is proximity-coupling-fed by an H-shaped slot etching in the ground. The center arm and two side arms of the H-shaped coupling slot are of dimensions $S_1 \times W_2$ and $S_2 \times W_2$, respectively. The H-shaped slot is placed parallel to the radial line of the circular patch, which keeps the current distribution of TM_{01} mode from being cut off by the slot. Using the proposed radial coupling slot is found to be effective in improving the isolation. Port 1 is excited through a 50-Ω microstrip transmission line on substrate 1, which has a tuning stub length of L_1.

From the circular cavity model [12], it is shown that the TM_{01} mode resonates at a frequency between TM_{21} and TM_{31} modes, which is about twice the resonant frequency of the fundamental TM_{11} mode. In order to make the two modes operate at an overlapped frequency range, a driven rod with a radius of R_3 and the capacitive feed technique are applied to shift down the resonant frequency of TM_{01} mode. The driven rod is soldered to the center of the circular patch, where an electric null exists when the circular patch operates in TM_{11} mode. This also ensures a good isolation between the two ports. The bandwidth can be broadened by increasing the size of the driven rod. Port 2 for TM_{01} mode is fed by another microstrip line with a quasi-circular stub, and a gradual broadband impedance transformation is achieved by tapering the width of the microstrip line. The quasi-circular stub is composed of a semicircular sheet with a radius of R_2 and a rectangular sheet with the dimensions $R_2 \times L_3$. The driven rod couples the electromagnetic energy to the radiating patch from the quasi-circular stub through an annular gap in the ground. This capacitive feed technique introduces capacitance to compensate for a portion of the inductance introduced by the driven rod while reducing the mainly resonant frequency of the conical TM_{01} mode. The shape of the quasi-circular stub is also used for advancing the radiation pattern characteristics of TM_{01} mode.

The impedance matching and optimum bandwidth of TM_{11} mode can be achieved by adjusting the dimensions of the H-shaped slot and the open stub length L_1. To minimize the antenna dimensions, the antenna parameters have been optimized. The geometrical parameters of the conformal dual-port diversity patch antenna are given in Table I.

At the same time, resonant frequency of TM_{01} mode can be approximately determined by the size of the circular patch R1 and the air gap thickness h. Fig. 2 shows the impedance matching and operating frequency of TM_{01} mode that can be tuned by the dimensions of the driven rod and the quasi-circular stub. The final design of the prototype antenna has the following parameters: $R_3 = 4.6$ mm, $R_2 = 5.8$ mm, $L_3 = 3$ mm.

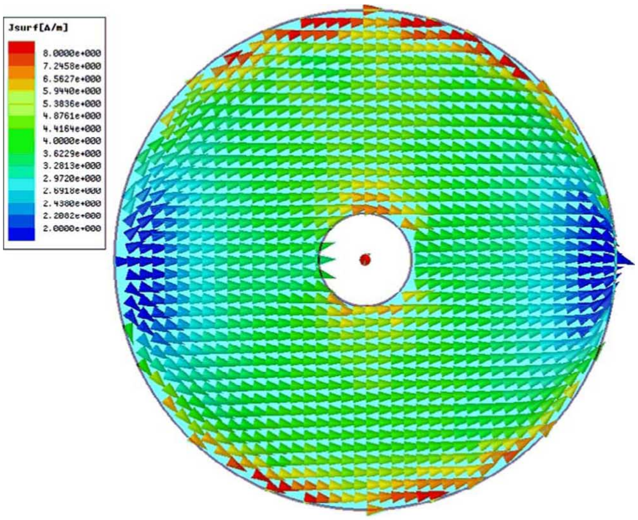

(a)

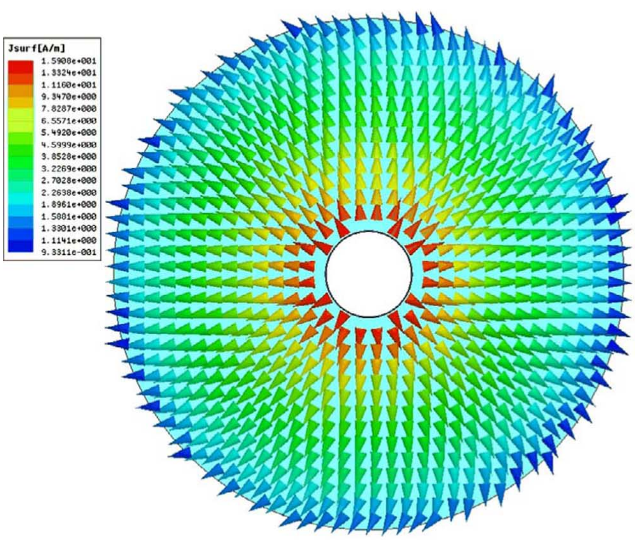

(b)

Fig. 3. Current distribution for (a) TM_{11} mode and (b) TM_{01} mode of the proposed antenna.

III. Simulation and Experimental Results

A. Current Distribution in the Circular Patch

The antenna was designed and simulated using Ansoft's HFSS full-wave simulator. Fig. 3 contains the current distribution for both TM_{11} and TM_{01} modes. It clearly shows the differences between the modes in terms of azimuthal angles. Currents in the case of TM_{11} mode have the same direction at both the top and bottom edges of the circular patch, giving a maximum radiation in the broadside, while they are along the radial direction of the patch in TM_{01} mode, and therefore this mode gives a null in the broadside. Consequently, these two modes with different radiation patterns are orthogonal to each other and provide hemispherical coverage. The current distribution of TM_{01} mode assuredly similar to the top-loaded monopole is invariable for all ϕ, so that the radiated field has only θ component as a typical monopole. However, due to the only 0.07-wavelength antenna height, the top-loaded monopole cannot be resonant due to the excessive loaded capacitance. This mode has the advantage of a lower profile than the conventional quarter-wavelength monopole antenna.

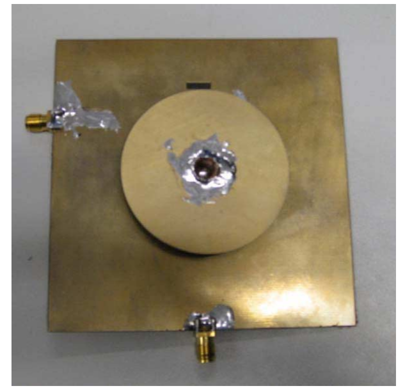

Fig. 4. Photograph of the constructed hybrid-fed patch antenna.

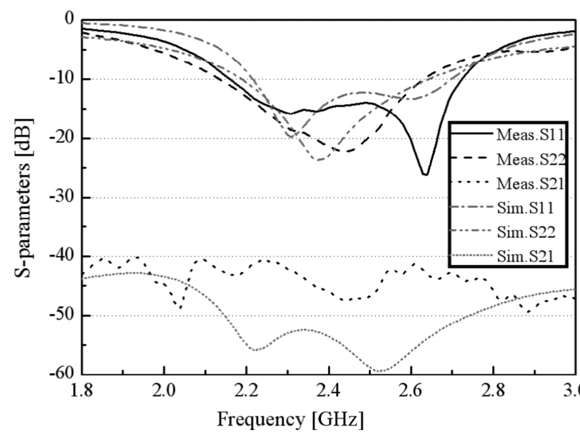

Fig. 5. Measured and simulated S-parameters of the proposed antenna.

B. Fabricated Prototype Results

To prove the design, a prototype of the proposed antenna has been fabricated and measured. Fig. 4 exhibits the photograph of the constructed prototype. Fig. 5 shows the measured and simulated S-parameters of the constructed prototype. The measured data in general agrees with the simulated results obtained from Ansoft simulation software High Frequency Structure Simulator (HFSS). It is observed that the bandwidths of -10 dB reflection coefficient are 560 MHz (2.16–2.72 GHz, 23.0%) and 500 MHz (2.14–2.64 GHz, 20.5%) for broadside TM_{11} mode and conical TM_{01} mode, respectively. The major challenge in designing the antenna is to tune the two resonant modes to resonate at the same frequency range. For this antenna, the overlapping frequency range that can excite both modes is from 2.16 to 2.64 GHz (19.7%). High isolation $(< -40\ \mathrm{dB})$ between the two feeding ports for the entire impedance bandwidth of the proposed antenna is achieved.

The measured and simulated antenna gain for operating frequencies within the impedance bandwidth is presented in Fig. 6. Over the bandwidth, the measured gain is about $7.1 \sim 9.1$ dBi for the broadside radiation and about $3.4 \sim 4.3$ dBi for the conical radiation. The slight decrease in antenna gain is mainly owing to the metallic loss and additional loss of the SMA

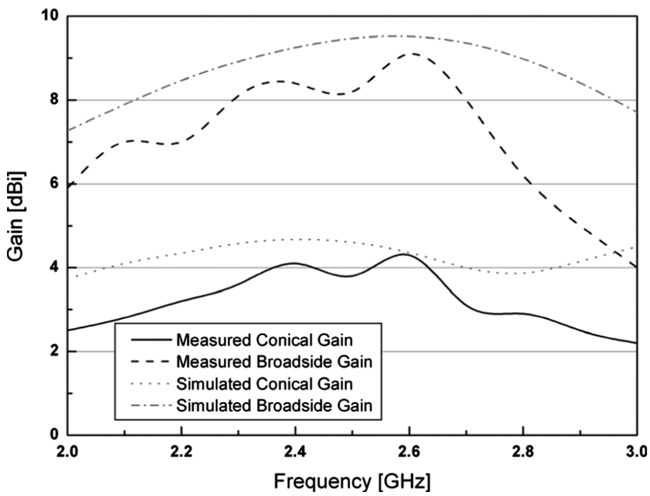

Fig. 6. Measured and simulated gain of the proposed antenna.

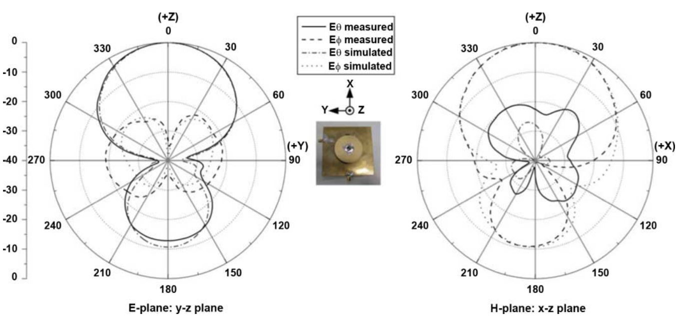

Fig. 7. Measured and simulated E- and H-plane patterns for broadside mode at 2.44 GHz.

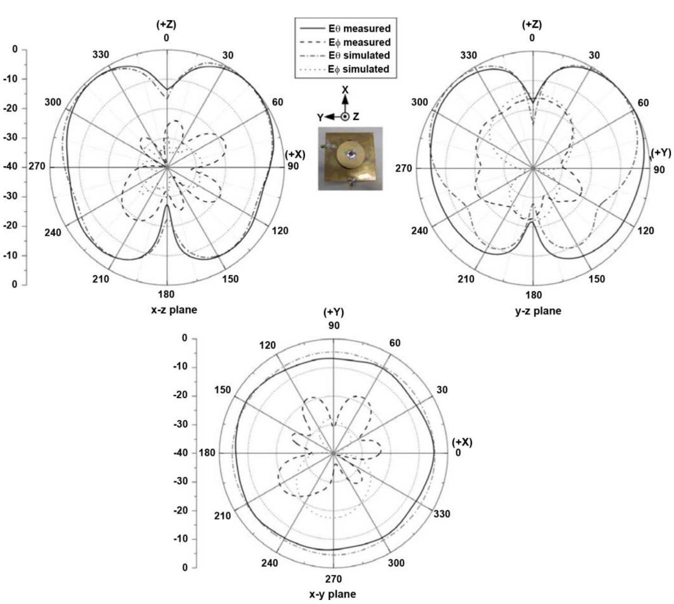

Fig. 8. Measured and simulated radiation patterns for conical mode at 2.44 GHz.

connectors and cables during the prototype construction and measurement.

Figs. 7 and 8 show the measured and simulated radiation patterns for both TM_{11} and TM_{01} modes at 2.44 GHz. When one port is being measured, the other port is terminated using a 50-Ω broadband load. It clearly shows that TM_{11} mode reveals good broadside radiation patterns and TM_{01} mode shows monopole-like radiation patterns. For the broadside TM_{11} mode, the main beam in the E-plane is toward the z-axis, which compensates for the radiation null of the monopole-like TM_{01} mode in the broadside direction. The cross-polarization levels are about -20 $-$dB. For the conical TM_{01} mode, the radiations in the azimuth plane are circular with small variation. The polarity of TM_{01} mode with conical radiation is orthogonal to that of broadside TM_{11} mode on the H-plane. The copolarization patterns in the elevation plane are symmetrical, while the cross-polarization levels are about -18 dB below the copolarization.

IV. Conclusion

A dual-port conformal diversity patch antenna with different radiation characteristics has been presented. The TM_{11} mode with broadside radiation is proximity-coupling-fed by an H-shaped slot, while a driven rod and the capacitive feed technique are applied to shift down the resonant frequency of TM_{01} mode. By making use of a hybrid feed network, the conical TM_{01} mode and the broadside TM_{11} mode of the antenna can be excited at an overlapped frequency band, which is attractive for providing hemispherical coverage for indoor mobile communication applications. From the measured results, it is found that the main-beam positions of the radiation patterns are directed at the elevation angles of 50° and 0° for both modes, respectively. This characteristic makes the antenna a good candidate for future pattern or polarization diversity applications in WLAN and multiple-input–multiple-output (MIMO) communications systems.

References

[1] W. K. Toh, Z. N. Chen, X. Qing, and T. S. P. See, "A planar UWB diversity antenna," *IEEE Trans. Antennas Propag.*, vol. 57, no. 11, pp. 3467–3473, Nov. 2009.
[2] X. Wang, Z. Feng, and K. M. Luk, "Pattern and polarization diversity antenna with high isolation for portable wireless devices," *IEEE Antennas Wireless Propag. Lett.*, vol. 8, pp. 209–211, 2009.
[3] I. J. Bahl and P. Bhartia*, Microstrip Antennas*. Norwood, MA: Artech House, 1980.
[4] H. Wong, K. L. Lau, and K. M. Luk, "Design of dual-polarized L-probe patch antenna arrays with high isolation," *IEEE Trans. Antennas Propag.*, vol. 52, no. 1, pp. 45–52, Jan. 2004.
[5] S. Gao and A. Sambell, "Dual-polarized broad-band patch antennas fed by proximity coupling," *IEEE Trans. Antennas Propag.*, vol. 53, no. 1, pp. 526–531, Jan. 2005.
[6] K. L. Wong and T. W. Chiou, "Broad-band dual-polarized patch antennas fed by capacitively coupled feed and slot-coupled feed," *IEEE Trans. Antennas Propag.*, vol. 50, no. 3, pp. 346–351, Mar. 2002.
[7] E. R. Iglesias, O. Q. Teruel, and M. S. Ferflifldez, "Compact multimode patch antennas for MIMO applications," *IEEE Antennas Propag. Mag.*, vol. 50, no. 2, pp. 197–205, Apr. 2008.
[8] V. G. Posadas, D. S. Vargas, E. R. Iglesias, J. L. V. Roy, and C. M. Pascual, "Approximate analysis of short circuited ring patch antenna working at TM_{01} mode," *IEEE Trans. Antennas Propag.*, vol. 54, no. 6, pp. 1875–1879, Jun. 2006.
[9] O. Q. Teruel and E. R. Iglesias, "Design of short-circuited ring-patch antennas working at TM_{01} mode based on neural networks," *IEEE Antennas Wireless Propag. Lett.*, vol. 5, pp. 559–562, 2006.
[10] S. L. S. Yang and K. M. Luk, "Design of a wide-band L-probe patch antenna for pattern reconfiguration or diversity applications," *IEEE Trans. Antennas Propag.*, vol. 54, no. 2, pp. 433–438, Feb. 2006.
[11] L. Economou and R. J. Langley, "Patch antenna equivalent to simple monopole," *Electron. Lett.*, vol. 33, no. 9, pp. 727–729, Nov. 1999.
[12] Y. S. Wu and F. J. Rosenbaum, "Mode chart for microstrip ring resonators," *IEEE Trans. Microw. Theory Tech.*, vol. MTT-21, no. 7, pp. 487–489, Jul. 1973.